HEFAT2014
10th International Conference on Heat Transfer, Fluid Mechanics and Thermodynamics
14 – 16 July 2014
Orlando, Florida

INVESTIGATION OF A TWO-PHASE FLOW NATURAL CIRCULATION LOOP WITH DIVERGENT MICROCHANNEL EVAPORATOR

Lee J.D.[1], Wu T.R.[2], Huang C.L.[2], Chao Y.C.[2] and Pan C.[2]*
[1] Nuclear Science and Technology Development Center,
[2] Department of Engineering and System Science,
National Tsing Hua University,
Hsinchu, 30013,
Taiwan

*Author for correspondence
E-mail: cpan@ess.nthu.edu.tw

ABSTRACT

The development of microelectronics is toward high performance, high efficiency and yet small size. Thermal management of microelectronics is of critical concern and significant interest. Microchannel boiling is an advanced cooling technology for high heat flux devices. The present study explores heat removal capability of a two-phase natural circulation loop with divergent microchannel evaporator. Our previous studies revealed that a diverging cross section design significantly could stabilize and enhance the heat transfer of flow boiling. The temperatures at the inlet and outlet of both evaporator and condensing units are measured to evaluate the heat removal capability of the loop. Moreover, the pressure changes through the downcomer and lower horizontal tube are both measured to deduce the flow rate through the loop based on the relationship between flow rate and pressure drop. This study uses the high speed video camera to capture the flow patterns in the evaporator and riser. The working fluid employed in the present study is ethanol, as its boiling temperature at atmospheric pressure is 78.4 ℃, which is below the temperature limit of the most microelectronic materials. The results show that the loop mass flow rate increases monotonically with increasing the heating power of the evaporator after boiling incipience. The current experimental results indicate that the highest base heat flux could achieve is about 105 kWm^{-2} with no sign of dry-out and it has great potential to reach a higher heat flux. Moreover, it is found that the loop instability appears at low heating powers after boiling begins, while it can be suppressed if the input power is higher than 20W. Indeed, the present two-phase natural circulation loop with divergent microchannel evaporator demonstrates stable circulation with high heat transfer capability.

INTRODUCTION

Cooling technologies have been rapidly developed to meet the challenge of thermal management for the microelectronics with high heat flux. Two-phase flow boiling in microchannels is an advanced cooling technology and has been one of the most promising methods. It has the advantages of the lowest pumping power, the highest efficiency and a high heat dissipation rate [1-2]. Therefore, studies of flow boiling characteristics in microchannels have been very active in recent years.

A micro-scale natural circulation loop with a microchannel evaporator is a passive heat removal device. The loop flow is driven by the buoyancy force created by the vapor produced in the evaporator. Such an innovative heat removal mechanism is an advanced cooling technology for high heat flux devices with an advantage of simplicity, low energy consumption and low cost. However, there are only limited studies in the literature. Hu and Tang [3] proposed a natural convection micro cooling system with a capillary microgroove evaporator. Experimental results indicated that the liquid fill ratio had a significant influence on thermal resistance and heat transfer in the cooling system. Increasing system's cooling capacity at higher input power was dependent on decreasing the thermal resistance between the outer surfaces of the condenser and ambient environment. The maximum heat dissipation capability of their micro cooling system had reached to 131.8 W.

Mukherjee and Mudawar [4-5] designed a compact cooling system of pumpless cooling loop. Their experiments were performed to explore the effects of boiler gap (separation distance between the boiling surface and opposite insulating wall) on cooling performance and critical heat flux (CHF) for water and FC-72. The gap was varied from 0.051 to 21.46 mm. For large gaps, CHF showed insignificant dependence on the

gap for both fluids. However, small gaps produced CHF variations that were both drastic and which followed opposite trends for the two fluids.

The present study develops a two-phase natural circulation loop with divergent microchannel evaporator. Our previous studies [6-9] demonstrated that a divergent microchannel design would stabilize the two-phase flow and enhance flow boiling heat transfer. The natural circulation loop consists of an evaporator with divergent microcahnnels, a riser, a downcomer and a condensing unit with a cooling tank cooled externally by cooling water. The present study experimentally examines two-phase flow characteristics and heat removal capability of this loop. The divergent microchannel evaporator employed in the present study is prepared by silicon bulk micromachining and anodic bonding procedures. The dynamic two-phase flow patterns are visualized using a high-speed digital CCD camera. The two phase flow characteristics are analyzed simultaneously by measuring the temperatures and pressure drops at the setting points in the loop.

NOMENCLATURE

A	[m^2]	Area
C_p	[$Jkg^{-1}K^{-1}$]	Constant pressure specific heat
D	[m]	Diameter
D_H	[m]	Hydraulic diameter
F	[-]	Frictional factor
g	[ms^{-2}]	Gravity acceleration
h_{fg}	[Jkg^{-1}]	Latent heat of evaporation
H	[m]	Height
K	[$Wm^{-1}K^{-1}$]	Thermal conductivity
L	[m]	length
$\dot{m}$	[kgs^{-1}]	Mass flow rate
ΔP	[Pa]	Pressure drop
$\dot{Q}$	[Ws^{-1}]	Heat transfer rate
q''	[Wm^{-2}]	Heat flux
R	[$W^{-1}K$]	Thermal resistance
Re	[-]	Reynolds number
T	[K]	Temperature
V	[ms^{-1}]	Velocity
W	[m]	Width

Special characters

ρ	[kgm^{-3}]	Density
Φ	[-]	Efficiency
μ	[$kgm^{-1}s^{-1}$]	Viscosity
δ	[N/m]	Surface tension

Subscripts

c	Condensing unit
co	Condensing tube
e	Evaporator
f	Liquid phase
g	Gas phase
H	Horizontal
i	Inlet of test section
loss	loss
m	Average
o	Outlet of test section
Py	Pyrex glass
p	PDMS
r	riser
sat	saturated
single	Single phase
t	Loop
total	total
two-phase	Two-phase
V	vertical
w	wall

EXPERIMENTAL DETAILS

1. Experimental Setup

Figure 1 illustrates the simple natural circulation loop with a microchannel evaporator. The microchannel evaporator, with a dimension of 20mm x 20mm, is made from a 4-inches silicon wafer. Through micro-fabrication processes, there are 18 parallel diverging microchannels with depth of 200 μm, length of 10.5 mm and the width of the diverging microchannel is from 250 μm to 350 μm. The channels are covered with Pyrex glass 7740 by anodic bonding to enable flow visualization. The riser is a circular tube with diameter of 4 mm and length of 150 mm. On the other hand, the vertical downcomer is also a circular tube with diameter of 4 mm and length of 190 mm. The lower horizontal part is a circular tube with diameter of 4 mm and length of 100 mm. The water cooled condensing unit consisting of a cooling tank with the working fluid of about 1 litter is similar to that employed by Mudawar and Mukherjee [4-5]. The temperature of the working fluid in the tank may be controlled by cooling water flow rate. For the present study, the cooling water is driven by HPLC pump and the flow rate is kept at 10 mL/min. The external tube with a diameter of 6 mm and a length of 700 mm is connected with experimental loop through the junction valve. This is functionally opened when the working fluid is filled into the experimental loop through a small hole on top of the cooling tank. This design is similar to the liquid supply flask of Mudawar and Mukherjee [4-5]. Table 1 displays the geometries of the two-phase natural circulation loop with divergent microchannel evaporator.

The microchannel evaporator is adhered on a heating module with silver glue to minimize thermal resistance. The heating module is a copper block heated by a cartridge heater with controllable power. To minimize heat loss, the whole block and the test section are insulated with Polydimethylsiloxane (PDMS) except the side surface of the evaporator for flow visualization.

To enable the filling in the working fluid, an external tube connected with the natural circulation loop through a junction valve between the upper vertical downcomer and lower horizontal tube is designed as shown in the Fig. 1.

The flow visualization system consists of a high-speed digital camera (PHOTRON FASTCAM-ultima APX) mounted with a micro-lens (OPTEM Zoom 125), a monitor and a personal computer. The frame rate was typically set at 6000

frame s^{-1} to capture the fast-changing flow pattern. An *x*–*y*–*z* mechanism installed with the test module holds the high-speed digital camera and micro-lens and provides the accurate position on the test plane (*x*–*y* plane) and focusing (*z*-direction).

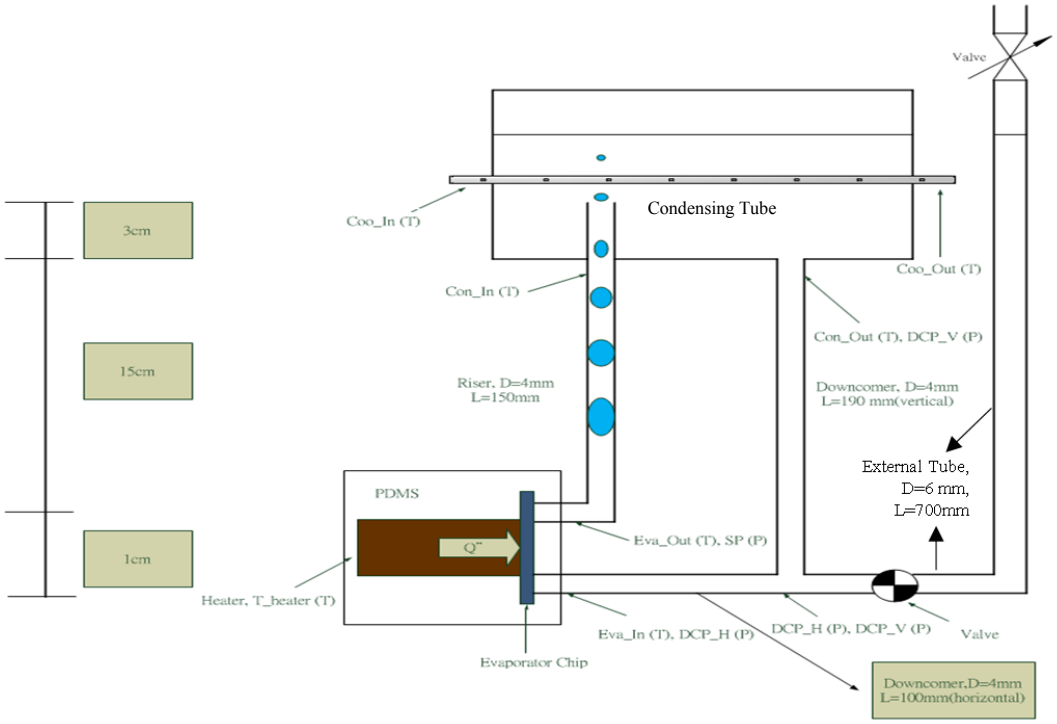

Figure 1 The design of the two-phase flow natural circulation loop with divergent microchannel evaporator

Table 1 The geometries of two-phase natural circulation loop with divergent microchannel evaporator

Evaporator size (mm × mm)	20×20	
The length of microchannel (mm)	10.5	
The depth of microchannel (μm)	200	
The width of microchannel in evaporator	Inlet (μm)	250
	Outlet (μm)	350
Riser	Diameter (mm)	4
	Length (mm)	150
Upper vertical downcomer	Diameter (mm)	4
	Length (mm)	190
Lower horizontal tube	Diameter (mm)	4
	Length (mm)	100
External Tube	Diameter (mm)	6
	Length (mm)	700

2. Experimental Procedure

2.1 Filling in the Working Fluid

The 95% ethanol is adopted as the working fluid. Its boiling temperature is about 78.4 ˚C at 1 atm. The working fluid is filled in the condensing tank through a small hole on the upper surface of the condensing tank with the junction valve connecting the external tube opened. When the setting level of 8 cm in height of the condensing tank is reached, the junction valve is closed again.

2.2 Setting the Heating Power

The experiment is started at a given heating power. For the present study, the input power of this natural circulation loop is ranged from 2W to 42W. The boiling incipience appears in this loop at about 8W.

2.3 The Measurement of Loop Flow Rate

The loop mass flow rate is evaluated based on the relationship between flow rate and pressure change through the downcomer and the pressure drop through the lower horizontal tube. For the present study, the loop flow rate is relatively small and the flow in the loop is firmed to be laminar. Therefore, the loop mass flow rate is related to the pressure drop through the lower horizontal tube as:

$$\dot{m}_H = \frac{\pi \rho D^4}{128 \mu L_H} \times \Delta P_H \qquad (1)$$

While it is related to the pressure change through the downcomer as:

$$\dot{m}_V = \frac{\pi \rho D^4}{128 \mu L_V} \times (\rho g L_V - \Delta P_V) \qquad (2)$$

using the measurement of pressure change through the lower horizontal tube (mass flow rate_H) or the upper downcomer (mass flow rate_V).

2.4 The Data Acquisition and Flow Pattern Visualization

The data acquisition system records the signals from eight thermocouples and pressure transducers after the system reaches the steady state. Under flow boiling conditions, the two-phase flow patterns in the evaporator test section and the riser section are both visualized and recorded with a frame rate, typically at 6000 fps. Another experiment at different heating power is conducted following the same procedure.

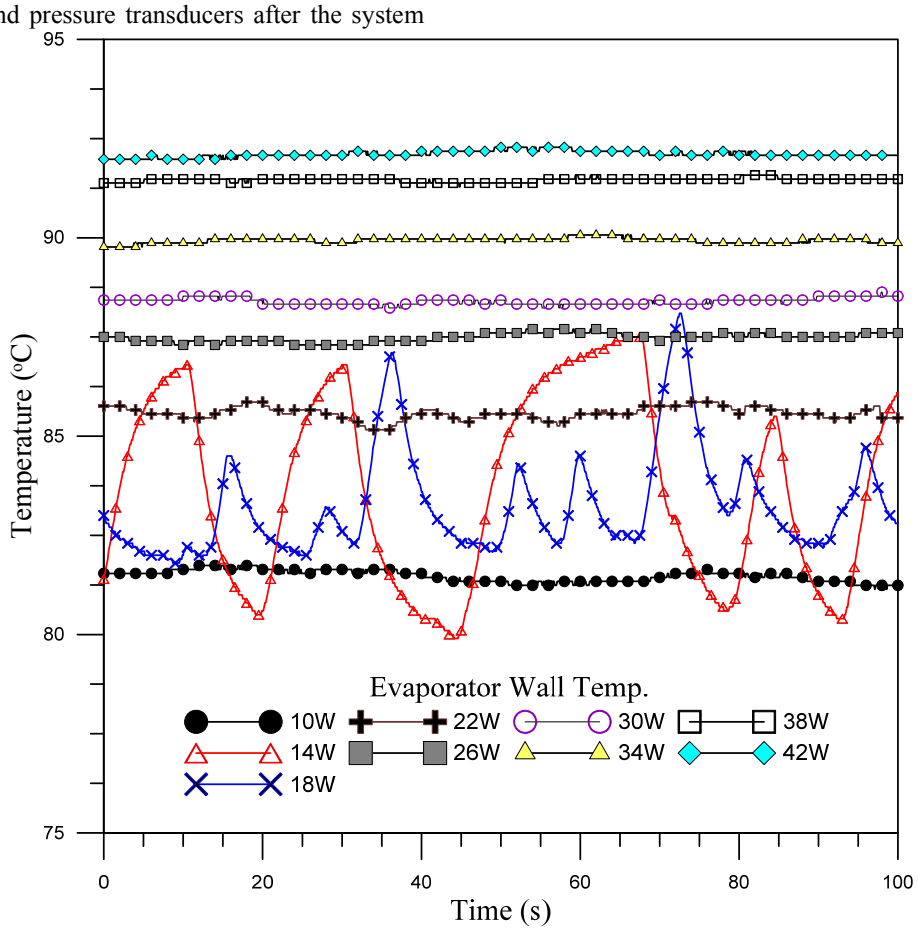

Figure 2 The heated wall temperature in the microchannel evaporator under different heating powers (t =0 refers a reference time after steady or quasi-steady state is reached.)

RESULTS AND DISCUSSION

1. Two-Phase Flow Patterns in the Microchannel Evaporator

Figure 2 illustrates that the heated wall temperature in the microchannel evaporator test section of the natural circulation loop under different heating powers. Fig. 2 together with the flow visualization reveal two types of flow boiling in the evapoartor under relatively low heating powers (< 24W). When the heating power is relatively low, the flow boiling appears only in the outlet of the evaporator and it cannot be visualized along the microchannels. This mild and stable flow boiling is accompanied with stable wall temperature. The other type is active flow boiling triggered by the increase in the heated power. As shown in the figure, if the heating power is greater or equal to 14 W, the flow instability appears and the wall temperature oscillates significantly. The magnitude of temperature oscillation for this case is about 8 ℃. Flow visualization reveals that the flow boiling prevails over the entire parallel microchannels intermittently. Such unstable flow persists as the heating power is further increased. The flow is stabilized again as the heating power is greater than or equal to 26 W.

For such high heating powers (≥26W), the flow boiling in the evaporator appears in the peripheral channels nearly symmetrically. Further increase in the heating power will start the boiling in central channels and flow boiling becomes more uniform over the entire evaporator. The flow patterns in the peripheral microchannels reveal a type of annular flow, possibly due to the less flow rate. In addition, the transition from the bubbly flow to annular flow may be observed in the central microchannels, possibly due to higher flow rate there. Significantly, Fig. 2 demonstrates very stable heated wall temperature during high power operation.

The unstable oscillations in the evaporator heated wall temperature at intermediate powers, as shown in Fig. 2, may be described as a type of flashing-induced instabilities. As reported in Furuya et al. [10] and Manera et al. [11], two types

of flashing-induced instability were recognized, the intermittent oscillation in high inlet subcooling and the sinusoidal oscillation in low inlet subcooling. In this study the inlet subcoolings of the evaporator test section are very high, and thus a type of intermittent boiling can be visualized during the two-phase boiling process at relatively low powers. The future work of the present study will be carried out by reducing the inlet subcoolings of the evaporator. The sinusoidal oscillations will be surveyed to support the estimation of flashing-induced instability.

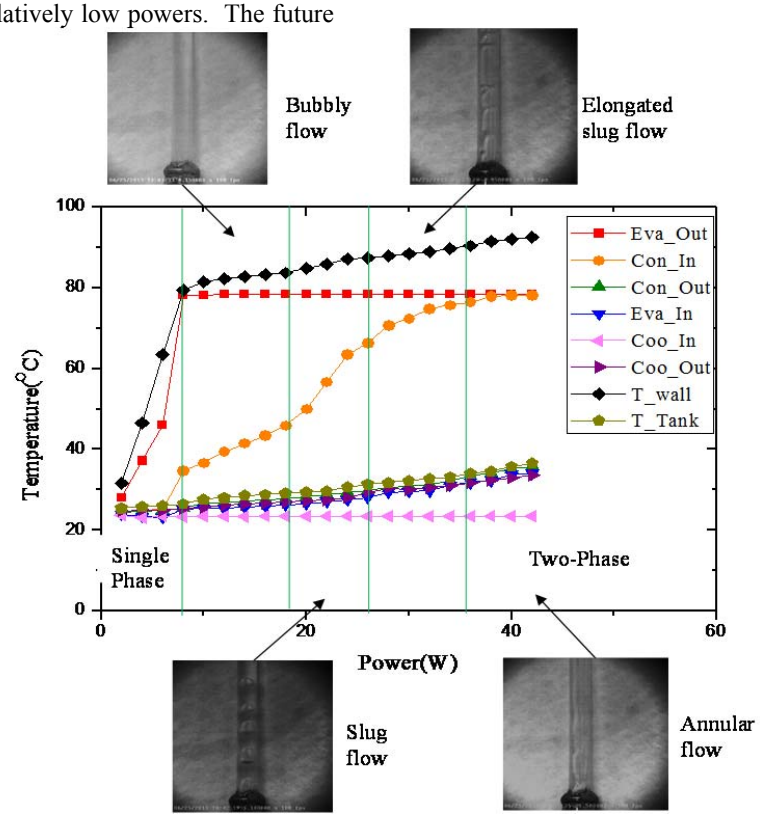

Figure 3 Mean temperatures at various locations in the loop and the corresponding two-phase flow patterns in the riser for various heating powers

2. Two-Phase Flow Patterns in the Riser

Figure 3 illustrates the mean temperatures at various locations in the loop and the corresponding two-phase flow patterns in the riser as a function of heating power. The figure indicates that boiling starts at a heating power of about 8W, at which the outlet temperature of the evaporator reaches saturation. The evaporator outlet temperature remains at the saturation temperature even for the highest heating power of this study. This indicates the non-dryout condition for the loop subject to the highest heating power (42W) in this study. The figure also indicates that, after boiling incipience, the temperature at the inlet of the condenser is substantially increased with the heating powers resulted from the much efficient flow boiling heat transfer in the evaporator and more heat is carried out by the loop flow and condensed near the inlet of the condenser.

In the low power region (8W≤q≤18W), the flow pattern in the riser is bubbly flow, as shown in Fig. 3. The type of flow pattern in the riser is affected by the intermittent active flow boiling in the evaporator at intermediate heating powers, as described in the preceding section. The single bubble is broken into small bubbles dispersed in the riser. This then results in the very obvious temperature oscillations at the inlet of the condenser, as shown in Fig. 4.

As the heating power is further increased to the range of 18W≤q≤26W, the flow pattern in the riser changes from bubbly flow into slug flow. In this region, the condenser inlet temperature demonstrates a greater slope indicating an even better heat transfer in the evaporator. On the other hand, the temperature oscillations at the inlet of the condenser is diminishing for q > 20W, as illustrated in Fig. 4, and the amplitude of oscillations approaches ± 1 ℃, as indicated in Fig. 5. This trend is consistent with the heated wall temperature oscillation in the evaporator, as shown earlier in Fig. 2. Consistent with the result of Fig. 2, Fig. 5 also suggests that the loop instability appears at low heating powers after boiling begins, while it diminished as the heating power is greater than 20W. This microchannel natural circulation loop demonstrates stable two-phase flow at high powers under study.

As the heating power is greater than 28W, the heat transfer capability of this natural circulation loop is hardly distinguished through the slope of the condenser inlet temperature, which is close to the saturation temperature. For this region with high heating power, the loop heat transfer capability may be deduced

from the temperature of the condensing tank, i.e., T_Tank. Figure 3 indicates that T_ tank is still slowly increasing in this high power region. This demonstrates that this loop still presents excellent heat transfer capability, as it should be. In this region, elongated slug flow or annular flow prevails in the riser.

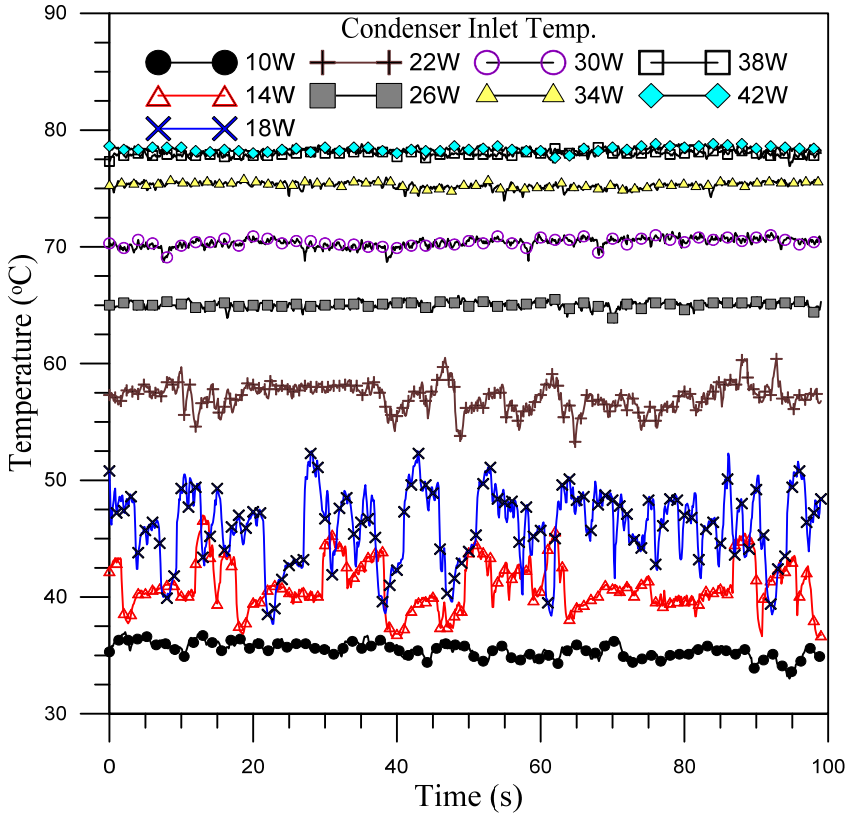

Figure 4 Temperature oscillations at the inlet of the condenser for various heating powers

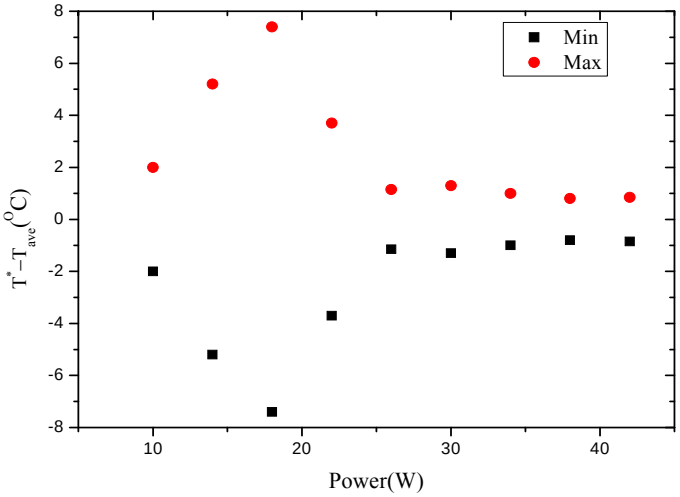

Figure 5 The amplitude of the temperature oscillation at the inlet of the condenser as the function of the heating power

3. The Analysis of Loop Mass Flow Rate

Figure 6 illustrates the loop mass flow rate versus the heating power of the evaporator obtained based on the measurement of pressure change through the lower horizontal tube (mass flow rate_H) or the downcomer (mass flow rate_V). The figure displays relatively good agreement between these two measurements. The results show that the

loop mass flow rate increases monotonically with increasing the heating power of the evaporator after boiling incipience. The positive slope demonstrates that buoyancy force created by the voids in the evaporator and riser is greater than the flow pressure drop around the loop. Such a behaviour is similar to that in a natural circulation loop with ordinary-sized channels in the evaporator. The increasing trend of loop mass flow rate based on the experimental results show that this microchannel natural circulation loop has a great potential to reach a higher heating power.

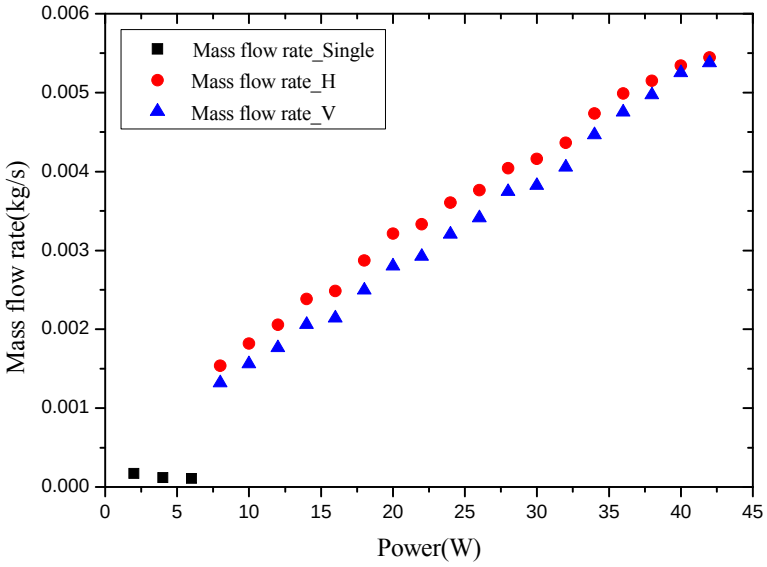

Figure 6 The loop mass flow rate versus the heating power of the evaporator based on the measurement of pressure change through the lower horizontal tube (mass flow rate_H) or the downcomer (mass flow rate_V). The pressure change in the single-phase region is too small to be accurately measured and data shown is probably inaccurate.

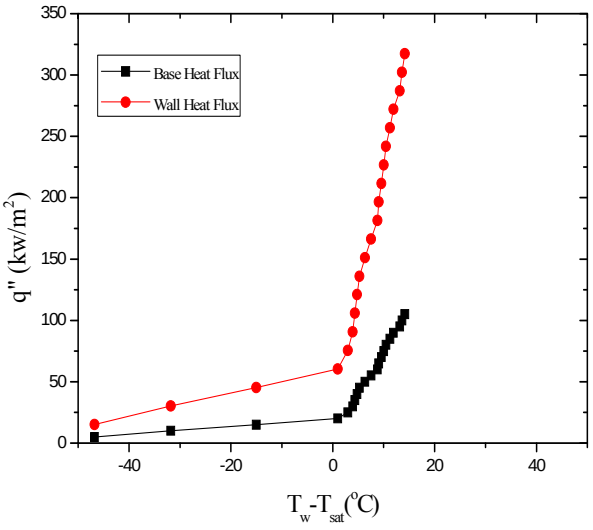

Figure 7 The boiling curve of the heat flux (q'') versus the heated wall superheat (T_w-T_{sat})

4. Boiling Curve

Figure 7 presents the boiling curve of the heat flux (q'') versus the wall superheat (T_W-T_{sat}). The steep slope in the figure demonstrates excellent heat transfer capability in the evaporator after boiling incipience, compared with that in the single-phase region. The current experimental results indicate that the highest base heat flux could achieve is about 105 kW/m^2 with no sign of dry-out and it has great potential to reach a higher heat flux. More experiments are now undergoing to explore critical power limit.

5. Heat Removal Efficiency of the Loop

Table 2 The heat removal efficiency of the loop for different input powers

Power (W)	Efficiency (%)	Power (W)	Efficiency (%)	Power (W)	Efficiency (%)
2	96.7	16	97.6	30	98.6
4	95.6	18	97.8	32	98.7
6	95.2	20	98.1	34	98.8
8	94.5	22	98.2	36	98.9
10	95.8	24	98.3	38	98.9
12	96.5	26	98.4	40	99.0
14	97.2	28	98.5	42	99.0

One of the major objectives of the present research is to evaluate the heat removal efficiency of the natural circulation loop with a divergent microchannel evaporator. The heat removal efficiency is defined as the ratio of the heat removal rate from the evaporator ($\dot{Q}_e$) divided by the input heating

power ($\dot{Q}_{total}$). Table 2 lists the heat removal efficiency of this loop for different input powers. The results demonstrate the excellent performance of the present loop. As a result of the whole heating block and the evaporator insulated with PDMS, the heat removal efficiency of this loop is ranged from 94.5% to 99%. After boiling starts, the heat removal efficiency increases with increasing input powers.

CONCLUSIONS

The present study investigates experimentally the heat transfer capability of a two-phase natural circulation loop with a divergent microchannel evaporator. The following conclusions may be drawn from the results of this study:

1. Two types of flow boiling may be observed in the evaporator at low powers: (1) the mild and stable flow boiling at the exit of the microchannel evaporator, and (2) the active and unstable flow boiling. Such unstable flow boiling is intermittent in nature and the temperature oscillation amplitude is about 8 ℃.
2. Depending on the heating power, the two-phase flow pattern in the riser could be bubbly, slug or annular flow.
3. In this study, the inlet subcoolings of the evaporator remain very high; the intermittent dramatic flow boiling may be caused by flashing-induced instabilities.
4. It is found that the loop instability appears at low heating powers after boiling starts, while it can be suppressed if the input power is higher than 20W. The present design of natural circulation loop with a divergent microchannel evaporator can effectively reduce the flow instability for low powers and can operate very stably for high powers.
5. The loop mass flow rate increases monotonically with increasing the heating power of evaporator after boiling incipience. The positive slope demonstrates that buoyancy force created by the voids in the evaporator and riser is greater than the flow pressure drop around the loop.
6. The present experimental results indicate that the highest base heat flux could achieve is about 105 kWm^{-2} with no sign of dry-out and it has great potential to reach a higher heat flux.

ACKNOWLEDGMENTS

This work was supported by the National Science Council of the Republic of China through contract NSC 100-2221-E-007-112-MY3.

REFERENCES

[1] Thome J. R., The new frontier in heat transfer: microscale and nanoscale technologies, *Heat Transfer Eng.* 27, 2006, pp. 1–3.

[2] Agostini B., Fabbri M., Park J. E., Wojtan L. and Thome J. R., State of the art of high heat flux cooling technologies, *Heat Transfer Eng.* 28, 2007, pp. 258–281.

[3] Hu X. and Tang D., Experimental investigation on flow and thermal characteristics of a micro phase- change cooling system with a microgroove evaporator, *International Journal of Thermal Sciences*,vol.46, 2007, pp.1163-1171.

[4] Mukherjee S. and Mudawar I., Smart, low-cost, pumpless loop for micro-channel electronic cooling using flat and enhanced surfaces, *Inter Society conference on Thermal Phenomena*, 2002, pp.360-370.

[5] Mukherjee S. and Mudawar I., Pumpless loop for narrow channel and micro-channel boiling, *Journal of Electronic Packaging*, vol.125, 2003, pp.431-441.

[6] Lu C.T. and Pan C., Bubble dynamics for convective boiling in silicon- based, converging and diverging microchannels, *Proc. 13th Int. Heat Transfer Conf.,* Sydney,Australia, 2006, pp.11.

[7] Lee P. C. and Pan C., Boiling heat transfer and two-phase flow of water in a single shallow microchannel with a uniform or diverging cross section, *J. Micromech. Microeng.* 18, 2008, 025005

[8] Lu C. T. and Pan C., Convective boiling in a parallel microchannel heat sink with a diverging cross section and artificial nucleation sites, *Experimental Thermal and Fluid Science*, vol.35, 2011, pp. 810-815.

[9] Lu C.T. and Pan C., A highly stable microchannel heat sink for convective boiling, *Journal of micromechanics and microengineering*, vol.19, 2009, pp. 055013.

[10] Furuya M., Inada F. and van der Hagen T.H.J.J., Flashing-induced density wave oscillations in a natural circulation BWR-mechanism of instability and stability map, *Nuclear Engineering and Design*, vol. 235, 2005, pp. 1557-1569.

[11] Manera A., Rohde U., Prasser H.-M. and van der Hagen T.H.J.J., Modeling of flashing- induced instabilities in the start-up phase of natural-circulation BWRs using the two-phase flow code FLOCAL, *Nuclear Engineering and Design*, vol.235, 2005, pp.1517-1535.

[12] Pan C., Two-phase flow and boiling heat transfer, 1 ed., Junjie Incorporated Company, Taipei, Taiwan, R.O.C., 2001. (in Chinese)